Inclusive electron scattering in a relativistic Green's function approach

Andrea Meucci, Franco Capuzzi, Carlotta Giusti, and Franco Davide Pacati
Dipartimento di Fisica Nucleare e Teorica, Università di Pavia and Istituto Nazionale di Fisica Nucleare, Sezione di Pavia, I-27100 Pavia, Italy

(Received 27 January 2003; published 2 May 2003)

A relativistic Green's function approach to the inclusive quasielastic (e,e') scattering is presented. The single-particle Green's function is expanded in terms of the eigenfunctions of the non-Hermitian optical potential. This allows one to treat final state interactions consistently in the inclusive and in the exclusive reactions. Numerical results for the response functions and the cross sections for different target nuclei and in a wide range of kinematics are presented and discussed in comparison with experimental data.

DOI: 10.1103/PhysRevC.67.054601 PACS number(s): 25.30.Fj, 24.10.Jv, 24.10.Cn

I. INTRODUCTION

The inclusive electron scattering in the quasielastic region addresses to the one-body mechanism as a natural interpretation. However, when the experimental data of the separation of the longitudinal and transverse responses were available, it became clear that the explanation of both responses necessitated a more complicated framework than the single-particle model coupled to one-nucleon knockout.

A review till 1995 of the experimental data and their possible explanations is given in Ref. [1]. Thereafter, only a few experimental papers were published [2,3]. New experiments with high experimental resolution are planned at JLab [4] in order to extract the response functions.

From the theoretical side, a wide literature was produced in order to explain the main problems raised by the separation, i.e., the lack of strength in the longitudinal response and the excess of strength in the transverse one. The more recent papers are mainly concerned with the contribution to the inclusive cross section of meson exchange currents and isobar excitations [5–7], with the effect of correlations [8,9], and the use of a relativistic framework in the calculations [7].

At present, however, the experimental data are not yet completely understood. A possible solution could be the combined effect of two-body currents and tensor correlations [8,10,11].

In this paper we want to discuss the effects of final state interactions in a relativistic framework. Final state interactions are an important ingredient of the inclusive electron scattering, since they are essential to explain the exclusive one-nucleon emission, which gives the main contribution to the inclusive reaction in the quasielastic region. The absorption in a given final state due, e.g., to the imaginary part of the optical potential produces a loss of flux which is appropriate for the exclusive process, but inconsistent for the inclusive one, where all the allowed final channels contribute and the total flux must be conserved.

This conservation is preserved in the Green's function approach considered here, where the components of the nuclear response are written in terms of the single-particle optical model Green's function. This result was originally derived by arguments based on the multiple scattering theory [12] and successively by means of the Feshbach projection operator formalism [13–16]. The spectral representation of the single-particle Green's function, based on a biorthogonal expansion in terms of the eigenfunctions of the non-Hermitian optical potential, allows one to perform explicit calculations and to treat final state interactions consistently in the inclusive and in the exclusive reactions. Important and peculiar effects are given, in the inclusive reactions, by the imaginary part of the optical potential, which is responsible for the redistribution of the strength among different channels.

In a previous paper of ours [15] the approach was used in a nonrelativistic framework to perform explicit calculations of the longitudinal and transverse inclusive response functions. The main goal of this paper is to extend the method to a relativistic framework and produce similar results. Although some differences and complications are due to the Dirac matrix structure, the formalism follows the same steps and approximations as those developed in the nonrelativistic framework of Refs. [15,16]. The numerical results obtained in the relativistic approach allow us to check the relevance of relativistic effects in the kinematics already considered in Ref. [15] and can be applied to a wider range of kinematics where the nonrelativistic calculations are not reliable.

In Sec. II the hadron tensor of the inclusive process is expressed in terms of the relativistic Green's function, which is reduced in Sec. III to a single-particle expression. The problem of antisymmetrization is discussed in Sec. IV. In Sec. V, the Green's function is calculated in terms of the spectral representation related to the optical potential. In Sec. VI, the results of the calculations are reported and compared with the experimental data. Summary and conclusions are drawn in Sec. VII.

II. THE GREEN'S FUNCTION APPROACH

A. Definitions and main properties

In the one-photon exchange approximation the inclusive cross section for the quasielastic (e,e') scattering on a nucleus is given [1] by

$$\sigma_{\mathrm{inc}}=K(2\varepsilon_{\mathrm{L}}R_{\mathrm{L}}+R_{\mathrm{T}}), \tag{1}$$

where K is a kinematical factor and

$$\varepsilon_{\mathrm{L}}=\frac{Q^2}{\boldsymbol{q}^2}\left(1+2\frac{\boldsymbol{q}^2}{Q^2}\tan^2(\vartheta_e/2)\right)^{-1} \tag{2}$$

measures the polarization of the virtual photon. In Eq. (2), ϑ_e is the scattering angle of the electron, $Q^2=\boldsymbol{q}^2-\omega^2$, and $q^\mu=(\omega,\boldsymbol{q})$ is the four-momentum transfer. All nuclear structure information is contained in the longitudinal and transverse response functions, R_L and R_T, defined by

$$R_\mathrm{L}(\omega,q)=W^{00}_\mathrm{tot}(\omega,q),$$
$$R_\mathrm{T}(\omega,q)=W^{11}_\mathrm{tot}(\omega,q)+W^{22}_\mathrm{tot}(\omega,q), \tag{3}$$

in terms of the diagonal components of the hadron tensor,

$$W^{\mu\mu}_\mathrm{tot}(\omega,q)=\int\sum_\mathrm{f}\ |\langle\Psi_\mathrm{f}|J^\mu(\boldsymbol{q})|\Psi_0\rangle|^2\,\delta(E_0+\omega-E_\mathrm{f}). \tag{4}$$

Here J^μ is the nuclear charge-current operator that connects the initial state $|\Psi_0\rangle$ of the nucleus, of energy E_0, with the final states $|\Psi_\mathrm{f}\rangle$, of energy E_f, both eigenstates of the $(A+1)$-body Hamiltonian H. The sum runs over the scattering states corresponding to all of the allowed asymptotic configurations and includes possible discrete states. As was done for $|\Psi_\mathrm{f}\rangle$, the degeneracy indexes will be omitted whenever they are unnecessary. The ground state $|\Psi_0\rangle$ is assumed to be nondegenerate. In order to avoid complications of little interest in the present context, we neglect recoil effects and consider only pointlike nucleons, without distinguishing between protons and neutrons. Unless stated otherwise, the wave functions are properly antisymmetrized.

The hadron tensor of Eq. (4) can equivalently be expressed as

$$W^{\mu\mu}_\mathrm{tot}(\omega,q)=-\frac{1}{\pi}\mathrm{Im}\langle\Psi_0|J^{\mu\dagger}(\boldsymbol{q})G(E_\mathrm{f})J^\mu(\boldsymbol{q})|\Psi_0\rangle, \tag{5}$$

where $E_\mathrm{f}=E_0+\omega$ and $G(E_\mathrm{f})$ is the Green's function related to H, i.e.,

$$G(E_\mathrm{f})=\frac{1}{E_\mathrm{f}-H+i\eta}. \tag{6}$$

Here and in all the equations involving G, the limit for $\eta\to+0$ is understood. It must be performed after calculating the matrix elements between normalizable states.

In this paper the interest is focused on relativistic wave functions for initial and final states. Therefore, the $(A+1)$-body Hamiltonian H is the sum of one-nucleon free Dirac Hamiltonians and two-nucleon interactions $V_{jj'}$, i.e.,

$$H=\sum_{j=1}^{A+1}(\boldsymbol{\alpha}_j\cdot\boldsymbol{p}_j+\beta_jM)+\frac{1}{2}\sum_{j,j'=1}^{A+1}V_{jj'}, \tag{7}$$

where the 4×4 Dirac matrices, $\boldsymbol{\alpha}_j$ and β_j, act on the bispinor variables of the nucleon j. No particular assumption is made on the 4×4 matrix structure of $V_{jj'}$.

In order to express the hadron tensor in terms of single-particle quantities, the same approximations as in the nonrelativistic case [15] are required. The first one consists in retaining only the one-body part of the charge-current operator J^μ. Thus, we set

$$J^\mu(\boldsymbol{q})=\sum_{i=1}^{A+1}j^\mu_i(\boldsymbol{q}), \tag{8}$$

where j^μ_i acts only on the variables of the nucleon i. By Eq. (8), one can express the hadron tensor as the sum of two terms, i.e.,

$$W^{\mu\mu}_\mathrm{tot}(\omega,q)=W^{\mu\mu}(\omega,q)+W^{\mu\mu}_\mathrm{coh}(\omega,q), \tag{9}$$

where $W^{\mu\mu}(\omega,q)$ is the incoherent hadron tensor [17], which contains only the diagonal contributions $j^{\mu\dagger}_iGj^\mu_i$, whereas the coherent hadron tensor $W^{\mu\mu}_\mathrm{coh}(\omega,q)$ gathers the residual terms of interference between different nucleons. As the incoherent hadron tensor, $W^{\mu\mu}_\mathrm{coh}(\omega,q)$ can be expressed in terms of single-particle quantities (see Sec. 9 of Ref. [16]), but for the transferred momenta considered in this paper, we can take advantage of the high-q approximation [18] and retain only $W^{\mu\mu}(\omega,q)$. This term can be further simplified using the symmetry of G for the exchange of nucleons and the antisymmetrization of $|\Psi_0\rangle$. Therefore, we write

$$W^{\mu\mu}_\mathrm{tot}(\omega,q)\simeq W^{\mu\mu}(\omega,q)=-\frac{A+1}{\pi}\times\mathrm{Im}\langle\Psi_0|j^{\mu\dagger}(\boldsymbol{q})G(E_\mathrm{f})j^\mu(\boldsymbol{q})|\Psi_0\rangle, \tag{10}$$

where $j^\mu(\boldsymbol{q})$ is the component of $J^\mu(\boldsymbol{q})$ related to an arbitrarily selected nucleon. Due to the well-known completeness property, i.e.,

$$\frac{1}{2\pi i}\int dE[G^\dagger(E)-G(E)]=1, \tag{11}$$

the incoherent hadron tensor fulfills the energy sum rule,

$$\int d\omega W^{\mu\mu}(\omega,q)=(A+1)\langle\Psi_0|j^{\mu\dagger}(\boldsymbol{q})j^\mu(\boldsymbol{q})|\Psi_0\rangle. \tag{12}$$

B. Projection operator formalism

This formalism yields an expression of the incoherent hadron tensor of Eq. (10) in terms of eigenfunctions and Green's functions of the optical potentials related to the various reaction channels. Apart from complications due to the Dirac matrix structure, we follow the same steps and approximations as in the nonrelativistic treatment [12,13,15,16].

Let us decompose H as

$$H=\boldsymbol{\alpha}\cdot\boldsymbol{p}+\beta M+U+H_R, \tag{13}$$

where $\boldsymbol{\alpha}\cdot\boldsymbol{p}+\beta M$ is the kinetic energy of an arbitrarily selected nucleon, U is the interaction between this nucleon and the other ones, and H_R is the residual Hamiltonian of A interacting nucleons. Such a decomposition cannot be performed in the physical space of the totally antisymmetrized $(A+1)$-nucleon wave functions. Therefore, we must operate in the Hilbert space $\mathcal{H}$ of the wave functions which are antisymmetrized only for exchanges of the nucleons of H_R.

This treatment is presented here only for the sake of simplicity. In Sec. IV we shall discuss its physical drawbacks and outline the necessary changes.

Let $|n\rangle$ and $|\varepsilon\rangle$ denote the antisymmetrized eigenvectors of H_R related to the discrete and continuous eigenvalues ε_n and ε, respectively. We introduce the operators P_n, projecting onto the n-channel subspace of $\mathcal{H}$, and Q_n, projecting onto the orthogonal complementary subspace, i.e.,

$$P_n = \sum_a \int d\boldsymbol{r} |\boldsymbol{r}a;n\rangle\langle n;\boldsymbol{r}a|,$$

$$Q_n = 1 - P_n. \tag{14}$$

Here $|\boldsymbol{r}a;n\rangle$ is the unsymmetrized vector obtained from the tensor product between the discrete eigenstate $|n\rangle$ of H_R, and the orthonormalized eigenvectors $|\boldsymbol{r}a\rangle$ $(a=1,2,3,4)$ of the position and the spin of the selected nucleon. The eigenvectors $|\boldsymbol{r}a\rangle$ have been chosen only for the sake of definiteness, as every complete orthonormalized set of single-nucleon vectors could define the same operators P_n. Apart from minor differences due to the present relativistic context, P_n and Q_n are the projection operators of the Feshbach unsymmetrized formalism [19]. Note, for later use, the relations

$$[P_n, \boldsymbol{\alpha}\cdot\boldsymbol{p} + \beta M] = 0,$$

$$H_R P_n = \varepsilon_n P_n. \tag{15}$$

Moreover, we introduce the projection operator into the continuous channel subspace, i.e.,

$$P_c = \int d\varepsilon \sum_a \int d\boldsymbol{r} |\boldsymbol{r}a;\varepsilon\rangle\langle\varepsilon;\boldsymbol{r}a|. \tag{16}$$

Due to the completeness of the set $\{|\boldsymbol{r}a;n\rangle, |\boldsymbol{r}a;\varepsilon\rangle\}$, one has

$$\sum_n P_n + P_c = 1. \tag{17}$$

Then, we insert Eq. (17) into Eq. (10) disregarding the contribution of P_c. This approximation, which simplifies the calculations, is correct for sufficiently high values of the transferred momentum q. Thus, the hadron tensor of Eq. (10) can be expressed as the sum

$$W^{\mu\mu}(\omega,q) = W^{\mu\mu}_{\mathrm{d}}(\omega,q) + W^{\mu\mu}_{\mathrm{int}}(\omega,q) \tag{18}$$

of a direct term,

$$W^{\mu\mu}_{\mathrm{d}}(\omega,q) = \sum_n W^{\mu\mu}_n(\omega,q),$$

$$W^{\mu\mu}_n(\omega,q) = -\frac{A+1}{\pi}\mathrm{Im}\langle\Psi_0|j^{\mu\dagger}(\boldsymbol{q})P_n G(E_{\mathrm{f}})P_n \times j^{\mu}(\boldsymbol{q})|\Psi_0\rangle, \tag{19}$$

and of a term

$$W^{\mu\mu}_{\mathrm{int}}(\omega,q) = \sum_n \hat{W}^{\mu\mu}_n(\omega,q),$$

$$\hat{W}^{\mu\mu}_n(\omega,q) = -\frac{A+1}{\pi}\mathrm{Im}\langle\Psi_0|j^{\mu\dagger}(\boldsymbol{q})P_n G(E_{\mathrm{f}})Q_n \times j^{\mu}(\boldsymbol{q})|\Psi_0\rangle, \tag{20}$$

which gathers the contributions due to the interference between the intermediate states $|\boldsymbol{r}a;n\rangle$ related to different channels.

We note that the interference term does not contribute to the energy sum rule. In fact, Eq. (11) yields

$$\int d\omega \hat{W}^{\mu\mu}_n(\omega,q) = (A+1)\langle\Psi_0|j^{\mu\dagger}(\boldsymbol{q})P_n Q_n j^{\mu}(\boldsymbol{q})|\Psi_0\rangle = 0. \tag{21}$$

Thus, the full contribution to the sum rule of the incoherent hadron tensor is given only by the direct term, i.e.,

$$\int d\omega W^{\mu\mu}(\omega,q) = \int d\omega W^{\mu\mu}_{\mathrm{d}}(\omega,q) = (A+1)\langle\Psi_0|j^{\mu\dagger}(\boldsymbol{q})\sum_n P_n j^{\mu}(\boldsymbol{q})|\Psi_0\rangle, \tag{22}$$

which, as a pure consequence of the omission of the continuous channels described by P_c, is smaller than the value of Eq. (12).

III. SINGLE-PARTICLE EXPRESSION OF THE HADRON TENSOR

A. Single-particle Green's functions

For the time being, we will disregard the effects of interference between different channels and consider only the direct contribution to the hadron tensor of Eq. (19). The matrix elements of $P_n G(E) P_n$ in the basis $|\boldsymbol{r}a;n\rangle$ define a single-particle Green's function $\mathcal{G}_n(E)$ having a 4×4 matrix structure, i.e.,

$$\langle\boldsymbol{r}a|\mathcal{G}_n(E)|\boldsymbol{r}'a'\rangle \equiv \langle n;\boldsymbol{r}a|G(E+\varepsilon_n)|\boldsymbol{r}'a';n\rangle. \tag{23}$$

Note that here the energy scale is in accordance with Ref. [16] and differs from Ref. [15].

The self-energy of $\mathcal{G}_n(E)$ is determined following the same steps used by Feshbach to determine the optical potential from the Schrödinger equation [19]. One starts from the relation

$$(E - \boldsymbol{\alpha}\cdot\boldsymbol{p} - \beta M - H_R - U + \varepsilon_n + i\eta)(P_n + Q_n) \times G(E+\varepsilon_n)P_n = P_n, \tag{24}$$

projects both sides by P_n and then by Q_n, uses Eqs. (15), resolves $Q_n G P_n$ in terms of $P_n G P_n$, and finally obtains

$$[E - \boldsymbol{\alpha}\cdot\boldsymbol{p} - \beta M - V_n(E) + i\eta]P_n G(E+\varepsilon_n)P_n = P_n, \tag{25}$$

with

$$V_n(E)=P_nUP_n+P_nUQ_n\frac{1}{E-Q_nHQ_n+\varepsilon_n+i\eta}Q_nUP_n. \tag{26}$$

Using Eq. (14) for P_n and considering the matrix elements in the basis $|\boldsymbol{r}a;n\rangle$ of both sides of Eq. (25), one has

$$\mathcal{G}_n(E)=\frac{1}{E-h_n(E)+i\eta}, \tag{27}$$

where

$$h_n(E)=\boldsymbol{\alpha}\cdot\boldsymbol{p}+\beta M+\mathcal{V}_n(E), \tag{28}$$

and $\mathcal{V}_n(E)$ has the 4×4 matrix structure defined by

$$\langle \boldsymbol{r}a|\mathcal{V}_n(E)|\boldsymbol{r}'a'\rangle \equiv \langle n;\boldsymbol{r}a|V_n(E)|\boldsymbol{r}'a';n\rangle. \tag{29}$$

Thus, $h_n(E)$ is the self-energy of the Green's function $\mathcal{G}_n(E)$, and $\mathcal{V}_n(E)$ is the related mean field. Using the same arguments as in the nonrelativistic case, one finds that $\mathcal{V}_n(E)$ is the unsymmetrized Feshbach optical potential [19], related to the channel n, for the relativistic Hamiltonian H.

Using the first equation in Eq. (14) and Eq. (23), the direct hadron tensor $W_n^{\mu\mu}(\omega,q)$ of Eq. (19) becomes

$$W_n^{\mu\mu}(\omega,q)=-\frac{1}{\pi}\lambda_n \mathrm{Im}\langle\varphi_n|j^{\mu\dagger}(\boldsymbol{q})\mathcal{G}_n(E_{\mathrm{f}}-\varepsilon_n)j^{\mu}(\boldsymbol{q})|\varphi_n\rangle, \tag{30}$$

where the initial state $|\varphi_n\rangle$, normalized to 1, is represented by the bispinor defined by the matrix elements,

$$\langle \boldsymbol{r}a|\varphi_n\rangle \equiv \sqrt{\frac{A+1}{\lambda_n}}\langle n;\boldsymbol{r}a|\Psi_0\rangle, \tag{31}$$

λ_n is the related spectral strength [20],

$$\lambda_n=(A+1)\sum_a\int d\boldsymbol{r}|\langle n;\boldsymbol{r}a|\Psi_0\rangle|^2, \tag{32}$$

with

$$\sum_n \lambda_n \simeq A+1. \tag{33}$$

The symbol $\langle f|g\rangle$ denotes the scalar product,

$$\langle f|g\rangle=\sum_a\int d\boldsymbol{r} f^*(\boldsymbol{r}a)g(\boldsymbol{r}a). \tag{34}$$

In Eq. (30) the hadron tensor is expressed in terms of single-particle quantities. As in the nonrelativistic case, $|\varphi_n\rangle$ are the eigenstates of the optical potential, i.e.,

$$[\boldsymbol{\alpha}\cdot\boldsymbol{p}+\beta M+\mathcal{V}_n(E_0-\varepsilon_n)]|\varphi_n\rangle=(E_0-\varepsilon_n)|\varphi_n\rangle. \tag{35}$$

If $|\Psi_E\rangle$ is the eigenstate of H corresponding asymptotically to a nucleon, of momentum $\boldsymbol{k}$, colliding with a target nucleus in the bound state $|\varepsilon_n\rangle$, the single-particle vectors $|\chi_n(E-\varepsilon_n)\rangle$ representing the elastic scattering wave functions $\langle n;\boldsymbol{r}a|\Psi_E\rangle$ are eigenstates of the same optical potential, i.e.,

$$[\boldsymbol{\alpha}\cdot\boldsymbol{p}+\beta M+\mathcal{V}_n(E-\varepsilon_n)]|\chi_n(E-\varepsilon_n)\rangle = (E-\varepsilon_n)|\chi_n(E-\varepsilon_n)\rangle. \tag{36}$$

Since E is the total energy $\sqrt{k^2+M^2}+\varepsilon_n$, the argument of $\mathcal{V}_n$ is the kinetic energy (including the rest mass) of the emitted nucleon.

B. Interference hadron tensor

The problem of expressing the interference hadron tensor $\hat{W}_n^{\mu\mu}$ in a one-body form is treated in Ref. [15] in the nonrelativistic context. It is argued that the contribution of $\hat{W}_n^{\mu\mu}$ can be included in the direct hadron tensor $W_n^{\mu\mu}$ by the simple replacement

$$\mathcal{G}_n(E)\rightarrow\mathcal{G}_n^{\mathrm{eff}}(E)\equiv\sqrt{1-\mathcal{V}_n'(E)}\mathcal{G}_n(E)\sqrt{1-\mathcal{V}_n'(E)}, \tag{37}$$

where $\mathcal{V}_n'(E)$ is the energy derivative of the Feshbach optical potential.

In Ref. [21], the problem is reconsidered from a rigorous viewpoint. The interference hadron tensor is expressed exactly as a series involving energy derivatives of $\mathcal{V}_n(E)$, of increasing order, plus a residual term which cannot be reduced to a single-particle form. The series is expected to rapidly converge near the quasielastic peak and at intermediate energies. It is argued that in this region of momenta and energies, the residual term is negligible. Thus, one recovers the result of Eq. (37) and second-order corrections, which do not seem to give a sizable contribution.

Neither the treatment nor the conclusions change if one considers the relativistic Hamiltonian H. Thus, for the hadron tensor of Eq. (18), we use the approximated expression obtained from Eq. (30) with the replacement (37),

$$W^{\mu\mu}(\omega,q)=-\frac{1}{\pi}\sum_n \lambda_n\mathrm{Im}\langle\varphi_n|j^{\mu\dagger}(\boldsymbol{q}) \times\mathcal{G}_n^{\mathrm{eff}}(E_{\mathrm{f}}-\varepsilon_n)j^{\mu}(\boldsymbol{q})|\varphi_n\rangle. \tag{38}$$

Since the interference term $\hat{W}_n^{\mu\mu}$ of Eq. (20) has no influence on the energy sum rule of the total hadron tensor of Eq. (18), a natural question arises whether the approximation leading to Eq. (38) may change the sum rule. Actually, one can observe that in Eq. (37), $\mathcal{G}_n(E)$ is modified by factors that neither change its properties of analyticity in the energy complex plane nor its high energy behavior. This fact is used in Ref. [15] to prove the relation

$$-\frac{1}{\pi}\int dE\ \mathrm{Im}\langle\boldsymbol{r}a|\mathcal{G}_n^{\mathrm{eff}}(E)|\boldsymbol{r}'a'\rangle = -\frac{1}{\pi}\int dE\ \mathrm{Im}\langle\boldsymbol{r}a|\mathcal{G}_n(E)|\boldsymbol{r}'a'\rangle=\delta(\boldsymbol{r}-\boldsymbol{r}')\,\delta_{aa'}. \tag{39}$$

Therefore, the energy sum rule obtained from Eq. (38) is exactly the same as in Eq. (22), i.e., the correct sum rule of the incoherent hadron tensor, apart from the contribution of the continuous channels.

C. Excited states of the residual nucleus

As neither microscopic nor empirical calculations are available for the optical potential $\mathcal{V}_n$ associated with the excited states $|\varepsilon_n\rangle$, a common practice relates them to the ground state potential $\mathcal{V}_0$ by means of an appropriate energy shift. Here, as in Ref. [15], we use the kinetic energy prescription for the shifts (see Sec. 5 of Ref. [16]), which is naturally suggested by the plane wave impulse approximation. Such a prescription preserves the value of the kinetic energy (including the rest mass), directly related to the value of the optical potential variable in the energy scale adopted here. Therefore we set

$$\mathcal{V}_n(E)\simeq\mathcal{V}_0(E), \tag{40}$$

which implies

$$\mathcal{G}_n(E)\simeq\mathcal{G}_0(E). \tag{41}$$

Using these approximations in Eq. (38), we write

$$W^{\mu\mu}(\omega,q)=-\frac{1}{\pi}\sum_n \lambda_n \mathrm{Im}\langle\varphi_n|j^{\mu\dagger}(\boldsymbol{q}) \times\mathcal{G}_0^{\mathrm{eff}}(E_{\mathrm{f}}-\varepsilon_n)j^{\mu}(\boldsymbol{q})|\varphi_n\rangle. \tag{42}$$

These approximations do not change the energy sum rule of $W^{\mu\mu}(\omega,q)$.

IV. ANTISYMMETRIZATION

For simplicity, the treatment of Secs. II and III was based on the unsymmetrized projection operator P_n defined in Eq. (14), leading to the Green's function $\mathcal{G}_n$ of Eq. (23). In this section we examine the drawbacks of this formulation and its possible alternatives. From a mathematical viewpoint, $\mathcal{G}_n$ deserves the name of Green's function since it fulfills sum rule (39), which is a qualifying property. Moreover, and intimately related, $\mathcal{G}_n$ is an invertible operator on the whole Hilbert space $\mathrm{L}^2(\mathbb{R}^3)$. Consequently, its self-energy is not affected by any undue restriction of domain and by the related mathematical problems.

Notwithstanding, the optical potential $\mathcal{V}_n$ related to $\mathcal{G}_n$ suffers from the drawback of having spurious eigenfunctions. In fact, H has both antisymmetrized and unsymmetrized eigenvectors $|\Psi_E\rangle$ and the latter ones generate eigenfunctions $\langle n;\boldsymbol{r}a|\Psi_E\rangle$ of $\mathcal{V}_n(E-\varepsilon_n)$, which have no physical meaning. No tool exists to make a distinction inside this unphysical degeneracy. Moreover, it is apparent that $\mathcal{V}_n$ cannot be compared with any empirical optical model potential.

The remedy is a treatment based on projection operators onto antisymmetrized states, although their inclusion into the hadron tensor is more laborious. Two approaches are available.

The first approach (see Sec. 3.2 of Ref. [16] and Appendix B of Ref. [15]) uses the Feshbach projection operator onto antisymmetrized states, i.e.,

$$P_n^{\mathrm{F}}=\sum_{a,a'}\int d\boldsymbol{r}d\boldsymbol{r}'\, a_{\mathbf{r}a}^{\dagger}|n\rangle\langle\boldsymbol{r}a|(1-K_n)^{-1}|\boldsymbol{r}'a'\rangle\langle n|a_{\mathbf{r}'a'}, \tag{43}$$

where $a_{\mathbf{r}a}^{\dagger}$ creates a nucleon in the state $|\boldsymbol{r}a\rangle$ and K_n is the one-body density matrix defined by

$$\langle\boldsymbol{r}a|K_n|\boldsymbol{r}'a'\rangle\equiv\langle n|a_{\mathbf{r}'a'}^{\dagger}a_{\mathbf{r}a}|n\rangle. \tag{44}$$

The results of the preceding section remain true with the replacement

$$\langle\boldsymbol{r}a|\mathcal{G}_n(E)|\boldsymbol{r}'a'\rangle\to\langle\boldsymbol{r}a|\mathcal{G}_n^{\mathrm{F}}(E)|\boldsymbol{r}'a'\rangle \equiv\sum_b\int d\boldsymbol{s}\langle n|a_{\mathbf{r}a}\frac{1}{E-H+\varepsilon_n+i\eta}a_{\mathbf{s}b}^{\dagger}|n\rangle \times\langle\boldsymbol{s}b|(1-K_n)^{-1}|\boldsymbol{r}'a'\rangle, \tag{45}$$

where $\mathcal{G}_n^{\mathrm{F}}$ is the Green's function related to the "symmetrized" Feshbach optical potential $\mathcal{V}_n^{\mathrm{F}}$ [22]. In this approach the spurious degeneracy disappears, since one operates in a Hilbert space of antisymmetrized states, but at the price of new drawbacks [16,23], namely, (1) $\mathcal{G}_n^{\mathrm{F}}$ is not fully invertible, and so in some cases it gives rise to incorrect Dyson equations; (2) both $\mathcal{G}_n^{\mathrm{F}}$ and $\mathcal{V}_n^{\mathrm{F}}$ are not symmetric for exchange $\boldsymbol{r}a\leftrightarrow\boldsymbol{r}'a'$, and therefore $\mathcal{V}_n^{\mathrm{F}}$ is non-Hermitian below the threshold of the inelastic processes; and (3) the usual nonlocal models of potential are probably inadequate for $\mathcal{V}_n^{\mathrm{F}}$, which shows a complicated nonlocal structure.

In short, the approach based on $\mathcal{V}_n^{\mathrm{F}}$ has nontrivial mathematical problems and it is not really useful, since this potential bears no close relation with the empirical optical model potential.

The second approach, where the above drawbacks disappear, is that of Ref. [16]. It is based on the extended projection operator of Ref. [24],

$$P_n^{(p+h)}=\sum_a\int d\boldsymbol{r}(a_{\mathbf{r}a}^{\dagger}+a_{\mathbf{r}a})|n\rangle\langle n|(a_{\mathbf{r}a}^{\dagger}+a_{\mathbf{r}a}), \tag{46}$$

which leads to

$$\langle\boldsymbol{r}a|\mathcal{G}_n(E)|\boldsymbol{r}'a'\rangle\to\langle\boldsymbol{r}a|\mathcal{G}_n^{(p+h)}(E)|\boldsymbol{r}'a'\rangle \equiv\langle n|a_{\mathbf{r}a}\frac{1}{E-H+\varepsilon_n+i\eta}a_{\mathbf{r}'a'}^{\dagger}|n\rangle +\langle n|a_{\mathbf{r}'a'}^{\dagger}\frac{1}{E+H-\varepsilon_n-i\eta}a_{\mathbf{r}a}|n\rangle. \tag{47}$$

$\mathcal{G}_n^{(p+h)}(E)$ is the full Green's function, including particle and hole contributions. It fulfills the sum rule of Eq. (39), is fully invertible, and produces mathematically correct Dyson equations. The related mean field $\mathcal{V}_n^{(p+h)}(E)$ has no spurious eigenfunctions corresponding to unsymmetrized states, and its properties of nonlocality and symmetry make it more easily comparable with the empirical optical model potentials. Therefore, we understand that in the following equations $\mathcal{G}_n$ will denote the full Green's function $\mathcal{G}_n^{(p+h)}$ of the relativistic Hamiltonian H. The associated mean field $\mathcal{V}_n$ is nonlocal as in the nonrelativistic case, and does not conserve the primarily 4×4 matrix structure of $V_{jj'}$.

V. SPECTRAL REPRESENTATION OF THE HADRON TENSOR

In this section we consider the spectral representation of the single-particle Green's function, which allows practical calculations of the hadron tensor of Eq. (42). In expanded form, it reads

$$W^{\mu\mu}(\omega,q) = -\frac{1}{\pi}\sum_n \lambda_n \mathrm{Im}\langle\varphi_n|j^{\mu\dagger}(\boldsymbol{q})\sqrt{1-\mathcal{V}'(E)} \times\mathcal{G}(E)\sqrt{1-\mathcal{V}'(E)}j^{\mu}(\boldsymbol{q})|\varphi_n\rangle, \tag{48}$$

where $E=E_{\mathrm{f}}-\varepsilon_n$. Here and below, the lower index 0 is omitted in the Green's functions and in the related quantities. According to the discussion of the preceding section, we understand that $\mathcal{G}$ is the full particle-hole Green's function of Eq. (47) and that $\mathcal{V}$ is the mean field potential related to $\mathcal{G}$ by the equations

$$\mathcal{G}(E)=\frac{1}{E-h(E)+i\eta}, \tag{49}$$

$$h(E)=\boldsymbol{\alpha}\cdot\boldsymbol{p}+\beta M+\mathcal{V}(E). \tag{50}$$

The use of this Green's function does not change the expressions of the normalized initial states $|\varphi_n\rangle$ and of the related spectroscopic factors λ_n, defined in Eqs. (31) and (32), respectively. Equivalently, they can be written as

$$\langle \boldsymbol{r}a|\varphi_n\rangle=\lambda_n^{-1/2}\langle n|a_{\mathbf{r}a}|\Psi_0\rangle, \tag{51}$$

$$\lambda_n=\sum_a\int d\boldsymbol{r}|\langle n|a_{\mathbf{r}a}|\Psi_0\rangle|^2. \tag{52}$$

Due to the complex nature of $\mathcal{V}(E)$, the spectral representation of $\mathcal{G}(E)$ involves a biorthogonal expansion in terms of the eigenfunctions of $h(E)$ and $h^\dagger(E)$. We consider the incoming wave scattering solutions of the eigenvalue equations, i.e.,

$$[\mathcal{E}-h^\dagger(E)]|\chi_{\mathcal{E}}^{(-)}(E)\rangle=0, \tag{53}$$

$$[\mathcal{E}-h(E)]|\tilde{\chi}_{\mathcal{E}}^{(-)}(E)\rangle=0. \tag{54}$$

The choice of incoming wave solutions is not strictly necessary, but it is convenient in order to have a closer comparison with the treatment of the exclusive reactions, where the final states fulfill this asymptotic condition and are the eigenfunctions $|\chi_E^{(-)}(E)\rangle$ of $h^\dagger(E)$.

The eigenfunctions of Eqs. (53) and (54) satisfy the biorthogonality condition

$$\langle\chi_{\mathcal{E}}^{(-)}(E)|\tilde{\chi}_{\mathcal{E}'}^{(-)}(E)\rangle=\delta(\mathcal{E}-\mathcal{E}'), \tag{55}$$

and, in absence of bound eigenstates, the completeness relation

$$\int_M^\infty d\mathcal{E}|\tilde{\chi}_{\mathcal{E}}^{(-)}(E)\rangle\langle\chi_{\mathcal{E}}^{(-)}(E)|=1, \tag{56}$$

where the nucleon mass M is the threshold of the continuum of $h(E)$.

Equations (55) and (56) are the mathematical bases for the biorthogonal expansions. The contribution of possible bound state solutions of Eqs. (53) and (54) can be disregarded in Eq. (56) since their effect on the hadron tensor is negligible at the energy and momentum transfers considered in this paper.

Inserting Eq. (56) into Eq. (49) and using Eq. (54), one obtains the spectral representation

$$\mathcal{G}(E)=\int_M^\infty d\mathcal{E}|\tilde{\chi}_{\mathcal{E}}^{(-)}(E)\rangle\frac{1}{E-\mathcal{E}+i\eta}\langle\chi_{\mathcal{E}}^{(-)}(E)|. \tag{57}$$

Therefore, Eq. (48) can be written as

$$W^{\mu\mu}(\omega,q)=-\frac{1}{\pi}\sum_n \mathrm{Im}\left[\int_M^\infty d\mathcal{E}\frac{1}{E_{\mathrm{f}}-\varepsilon_n-\mathcal{E}+i\eta} \times T_n^{\mu\mu}(\mathcal{E},E_{\mathrm{f}}-\varepsilon_n)\right], \tag{58}$$

where

$$T_n^{\mu\mu}(\mathcal{E},E)=\lambda_n\langle\varphi_n|j^{\mu\dagger}(\boldsymbol{q})\sqrt{1-\mathcal{V}'(E)}|\tilde{\chi}_{\mathcal{E}}^{(-)}(E)\rangle \times\langle\chi_{\mathcal{E}}^{(-)}(E)|\sqrt{1-\mathcal{V}'(E)}j^{\mu}(\boldsymbol{q})|\varphi_n\rangle. \tag{59}$$

The limit for $\eta\to+0$, understood before the integral of Eq. (58), can be calculated exploiting the standard symbolic relation

$$\lim_{\eta\to0}\frac{1}{E-\mathcal{E}+i\eta}=\mathcal{P}\left(\frac{1}{E-\mathcal{E}}\right)-i\pi\delta(E-\mathcal{E}), \tag{60}$$

where $\mathcal{P}$ denotes the principal value of the integral. Therefore, Eq. (58) reads

$$W^{\mu\mu}(\omega,q)=\sum_n\left[\mathrm{Re}T_n^{\mu\mu}(E_{\mathrm{f}}-\varepsilon_n,E_{\mathrm{f}}-\varepsilon_n) -\frac{1}{\pi}\mathcal{P}\int_M^\infty d\mathcal{E}\frac{1}{E_{\mathrm{f}}-\varepsilon_n-\mathcal{E}}\,\mathrm{Im}T_n^{\mu\mu}(\mathcal{E},E_{\mathrm{f}}-\varepsilon_n)\right], \tag{61}$$

which separately involves the real and imaginary parts of $T_n^{\mu\mu}$.

Some remarks on Eqs. (59) and (61) are in order. Let us examine the expression of $T_n^{\mu\mu}(\mathcal{E},E)$ at $\mathcal{E}=E=E_{\rm f}-\varepsilon_n$ for a fixed *n*. This is the most important case since it appears in the first term in the right hand side of Eq. (61), which gives the main contribution. Disregarding the square root correction, due to interference effects, one observes that in Eq. (59) the second matrix element (with the inclusion of $\sqrt{\lambda_n}$) is the transition amplitude for the single-nucleon knockout from a nucleus in the state $|\Psi_0\rangle$ leaving the residual nucleus in the state $|n\rangle$. The attenuation of its strength, mathematically due to the imaginary part of $\mathcal{V}^{\dagger}$, is related to the flux lost towards the channels different from *n*. In the inclusive response this attenuation must be compensated by a corresponding gain due to the flux lost, towards the channel *n*, by the other final states asymptotically originated by the channels different from *n*. In the description provided by the spectral representation of Eq. (61), the compensation is performed by the first matrix element in the right-hand side of Eq. (59), where the imaginary part of $\mathcal{V}$ has the effect of increasing the strength. Similar considerations can be made, on purely mathematical grounds, for the integral of Eq. (61), where the amplitudes involved in $T_n^{\mu\mu}$ have no evident physical meaning as $\mathcal{E}\neq E_{\rm f}-\varepsilon_n$. We want to stress here that in the Green's function approach it is just the imaginary part of $\mathcal{V}$, which accounts for the redistribution of the strength among different channels.

The matrix elements in Eq. (59) contain the mean field $\mathcal{V}(E)$ and its Hermitian conjugate $\mathcal{V}^{\dagger}(E)$, which are nonlocal operators with a possibly complicated matrix structure. Neither microscopic nor empirical calculations of $\mathcal{V}(E)$ are available. In contrast, phenomenological optical potentials are available. They are obtained from fits to experimental data, are local, and involve scalar and vector components only. The necessary replacement of the mean field by the empirical optical model potential is, however, a critical step.

In the nonrelativistic treatment of Refs. [15,21], this replacement is justified on the basis of the approximated equation (holding for every state $|\psi\rangle$)

$$\begin{aligned}&\mathrm{Im}\langle\psi|\sqrt{1-\mathcal{V}'(E)}\,\mathcal{G}(E)\,\sqrt{1-\mathcal{V}'(E)}|\psi\rangle\\&\quad\simeq\mathrm{Im}\langle\psi|\sqrt{1-\mathcal{V}_{\rm L}'(E)}\,\mathcal{G}_{\rm L}(E)\,\sqrt{1-\mathcal{V}_{\rm L}'(E)}|\psi\rangle,\end{aligned}\tag{62}$$

where $\mathcal{V}_{\rm L}(E)$ is the local phase-equivalent potential identified with the phenomenological optical model potential and $\mathcal{G}_{\rm L}(E)$ is the related Green's function. In Ref. [21], the proof of Eq. (62) is based on two reasons: (1) a model of $\mathcal{V}(E)$ commonly used in dispersion relation analyses; and (2) the combined effect of the factor $\sqrt{1-\mathcal{V}'(E)}$ and of the Perey factor, which connects the eigenfunctions of $\mathcal{V}(E)$ and $\mathcal{V}_{\rm L}(E)$. We stress that it is just the factor $\sqrt{1-\mathcal{V}'(E)}$, introduced to account for interference effects, which allows the replacement of $\mathcal{V}(E)$ by $\mathcal{V}_{\rm L}(E)$.

Although the Perey effect is not sufficiently known for the Dirac equation, we have a reasonable confidence that Eq. (62) holds also in the present relativistic context. Therefore, we insert Eq. (62) into Eq. (48). Then, all the developments of this section can be repeated with the simple replacement of $\mathcal{V}(E)$ by $\mathcal{V}_{\rm L}(E)$.

VI. RESULTS AND DISCUSSION

The cross sections and the response functions of the inclusive quasielastic electron scattering are calculated from the single-particle expression of the coherent hadron tensor in Eq. (61). After the replacement of the mean field $\mathcal{V}(E)$ by the empirical optical model potential $\mathcal{V}_{\rm L}(E)$, the matrix elements of the nuclear current operator in Eq. (59) (which represent the main ingredients of the calculation) are of the same kind as those giving the transition amplitudes of the electron induced nucleon knockout reaction in the relativistic distorted wave impulse approximation (RDWIA) [25]. Thus, the same treatment can be used as that which was successfully applied to describe exclusive $(e,e'p)$ and (γ,p) data [25,26].

The final wave function is written in terms of its upper component following the direct Pauli reduction scheme, i.e.,

$$\chi_{\mathcal{E}}^{(-)}(E)=\begin{pmatrix}\Psi_{\rm f+}\\ \dfrac{1}{M+\mathcal{E}+S^{\dagger}(E)-V^{\dagger}(E)}\boldsymbol{\sigma}\cdot\boldsymbol{p}\Psi_{\rm f+}\end{pmatrix},\tag{63}$$

where $S(E)$ and $V(E)$ are the scalar and vector energy-dependent components of the relativistic optical potential for a nucleon with energy E [27]. The upper component $\Psi_{\rm f+}$ is related to a Schrödinger equivalent wave function $\Phi_{\rm f}$ by the Darwin factor, i.e.,

$$\Psi_{\rm f+}=\sqrt{D_{\mathcal{E}}^{\dagger}(E)}\Phi_{\rm f},\tag{64}$$

$$D_{\mathcal{E}}(E)=1+\frac{S(E)-V(E)}{M+\mathcal{E}}.\tag{65}$$

$\Phi_{\rm f}$ is a two-component wave function which is the solution of a Schrödinger equation containing equivalent central and spin-orbit potentials obtained from the scalar and vector potentials [28,29].

As no relativistic optical potentials are available for the bound states, the wave function φ_n is taken as the Dirac-Hartree solution of a relativistic Lagrangian containing scalar and vector potentials [30,31].

Concerning the nuclear current operator, no unambiguous approach exists for dealing with off-shell nucleons. In the present calculations we use [32–34]

$$j_{\rm cc2}^{\mu}=F_1(Q^2)\gamma^{\mu}+i\frac{\kappa}{2M}F_2(Q^2)\sigma^{\mu\nu}q_{\nu},\tag{66}$$

where κ is the anomalous part of the magnetic moment, F_1 and F_2 are the Dirac and Pauli nucleon form factors, which are taken from Ref. [35], and $\sigma^{\mu\nu}=(i/2)[\gamma^{\mu},\gamma^{\nu}]$.

Current conservation is restored by replacing the longitudinal current [33] by

$$J^{\mathrm{L}}=J^{z}=\frac{\omega}{|\boldsymbol{q}|}\,J^{0}\;. \tag{67}$$

The calculations have been performed with the same bound state wave functions and optical potentials as in Refs. [25,26], where the RDWIA was able to reproduce $(e,e'p)$ and (γ,p) data.

The relativistic bound state wave functions have been obtained from the code of Ref. [30], where relativistic Hartree-Bogoliubov equations are solved in the context of a relativistic mean field theory to reproduce single-particle properties of several spherical and deformed nuclei [31]. The scattering state is calculated by means of the energy-dependent and A-dependent (EDAD1) complex phenomenological optical potential of Ref. [27], which is fitted to proton elastic scattering data on several nuclei in an energy range up to 1040 MeV.

In the calculations, the residual nucleus states $|n\rangle$ are restricted to single-particle one-hole states in the target. A pure shell model is assumed for the nuclear structure, i.e., we take a unitary spectral strength for each single-particle state, and the sum runs over all the occupied states.

The results presented in the following contain the contributions of both terms in Eq. (61). The calculation of the second term, which requires integration over all the eigenfunctions of the continuum spectrum of the optical potential, is a rather complex task. This term was neglected in the nonrelativistic investigation of Ref. [15], where its contribution was estimated to be very small. In the present relativistic calculations the effect of this term can be significant, and it is therefore included in the results.

A. The R_{L} and R_{T} response functions

The longitudinal and transverse response functions for ^{12}C at $q=400$ MeV/c are displayed in Fig. 1 and compared with the Saclay data [36]. The low energy transfer values are not given because the relativistic optical potentials are not available at low energies.

The agreement with the data is generally satisfactory for the longitudinal response. In contrast, the transverse response is underestimated. This is a systematic result of the calculations, and was also found in the nonrelativistic approach of Ref. [15]. It may be attributed to physical effects that are not considered in the single-particle Green's function approach, e.g., meson exchange currents.

The effect of the integral in Eq. (61) is also displayed. Its contribution is important and essential to reproduce the experimental longitudinal response.

As explained in Sec. III, the contribution arising from interference between different channels, see Eqs. (37) and (62), gives rise to the factor

$$\sqrt{1-\mathcal{V}_{\mathrm{L}}'(E)}=\sqrt{1-\beta S'(E)-V'(E)}. \tag{68}$$

We see, however, that here it gives only a slight contribution, due to a compensation between the energy derivatives $S'(E)$ and $V'(E)$.

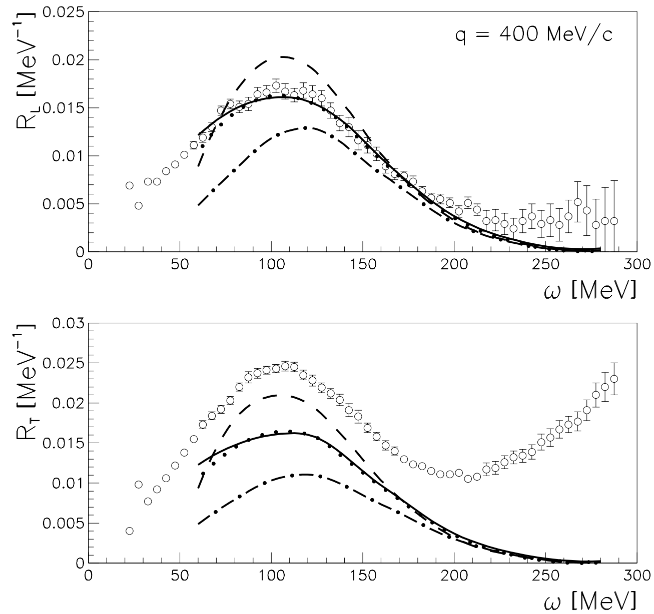

FIG. 1. Longitudinal (upper panel) and transverse (lower panel) response functions for the ^{12}C(e,e') reaction at $q=400$ MeV/c. Solid and dotted lines represent the NLSH results with and without the inclusion of the factor in Eq. (68), respectively. Dashed lines give the result without the integral in Eq. (61). Dot-dashed lines are the contribution of integrated single-nucleon knockout only. The data are from Ref. [36].

The contribution from all the integrated single-nucleon knockout channels is also drawn in Fig. 1. It is significantly smaller than the complete calculation. The reduction, which is larger at lower values of ω, gives an indication of the relevance of inelastic channels.

For the calculations in Fig. 1, the Hartree-Bogoliubov equations for the single-particle bound states have been solved using the set of the parameters of the relativistic mean field theory Larangian, which was called NLSH in Ref. [31]. In Fig. 2 a comparison is shown between the results obtained with this choice of parameters and the one called NL3 [31]. The shapes of the responses calculated with the different bound states show small differences. Their integrals must remain unchanged, according to the fact that the sum rule has to be preserved.

An example of the comparison between the results of our relativistic approach and those of the nonrelativistic one of Ref. [15] is presented in Fig. 3 for the longitudinal response function of ^{12}C at $q=400$ MeV/c. In the nonrelativistic calculations, the hole states and the optical potentials are taken from Refs. [37,38], respectively. Both complete relativistic and nonrelativistic calculations are in satisfactory agreement with the data. This result, however, is due to a different effect of the various contributions in the two approaches. In the nonrelativistic case, the interference between different channels produces a factor similar to that of Eq. (68), i.e.,

$$\sqrt{1-\mathcal{V}_{\mathrm{L}}'(E)}=\sqrt{1-V_{\mathrm{nr}}'(E)}, \tag{69}$$

where $V_{\mathrm{nr}}(E)$ is the nonrelativistic optical potential. This factor gives a substantial reduction that is necessary to reproduce the longitudinal response function. The integral in Eq. (61) gives only a small contribution, and is neglected. In the

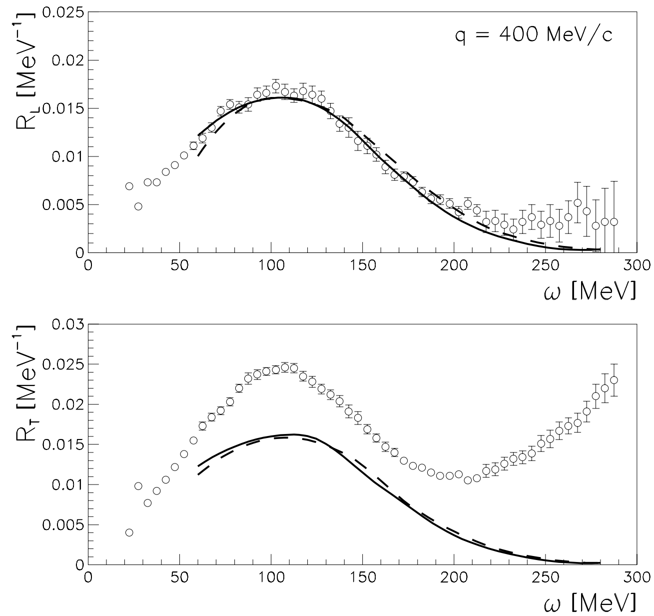

FIG. 2. Longitudinal (upper panel) and transverse (lower panel) response functions for the $^{12}C(e,e')$ reaction at $q = 400$ MeV/c. Solid lines represent the NLSH results, and dashed lines the NL3 results. Data as in Fig. 1.

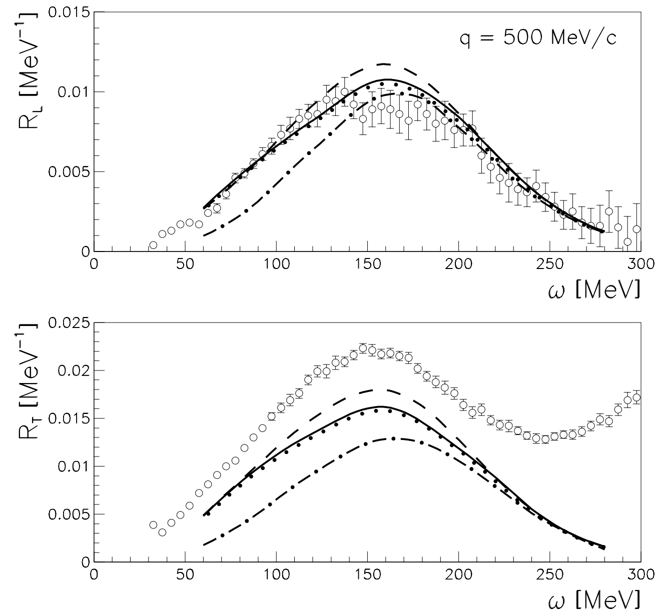

FIG. 4. The same as in Fig. 1, but for $q = 500$ MeV/c. The data are from Ref. [36].

relativistic approach, the factor of Eq. (68) is generally negligible, while the integral in Eq. (61) is essential to reproduce the experimental data.

The longitudinal and transverse response functions for ^{12}C at $q = 500$ and 600 MeV/c are displayed in Figs. 4 and 5, respectively, and are compared with the Saclay data [36]. The bound state wave functions have been obtained with the NLSH parametrization. As already found in Fig. 1 at $q = 400$ MeV/c, a good agreement with the data is obtained in both cases for the longitudinal response, while the transverse response is underestimated. Also in Figs. 4 and 5, only a slight effect is given by the factor in Eq. (68) arising from the interference between different channels. The role of the integral in Eq. (61) decreases on increasing the momentum transfer. At $q = 500$ MeV/c, its contribution is smaller than at $q = 400$ MeV/c, but still important to reproduce the experimental longitudinal response, while at $q = 600$ MeV/c

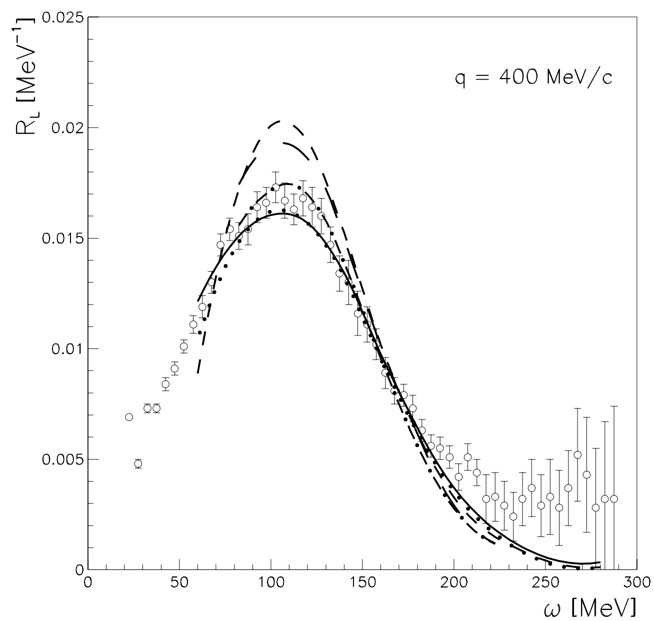

FIG. 3. Longitudinal response functions for the $^{12}C(e,e')$ reaction at $q = 400$ MeV/c. Solid and dotted lines represent the NLSH results with and without the inclusion of the factor in Eq. (68), respectively. Dashed line gives the result without the integral in Eq. (61). Dot-dashed and long-dashed lines are the nonrelativistic results of Ref. [15] with and without the inclusion of the factor in Eq. (69), respectively. Data as in Fig. 1.

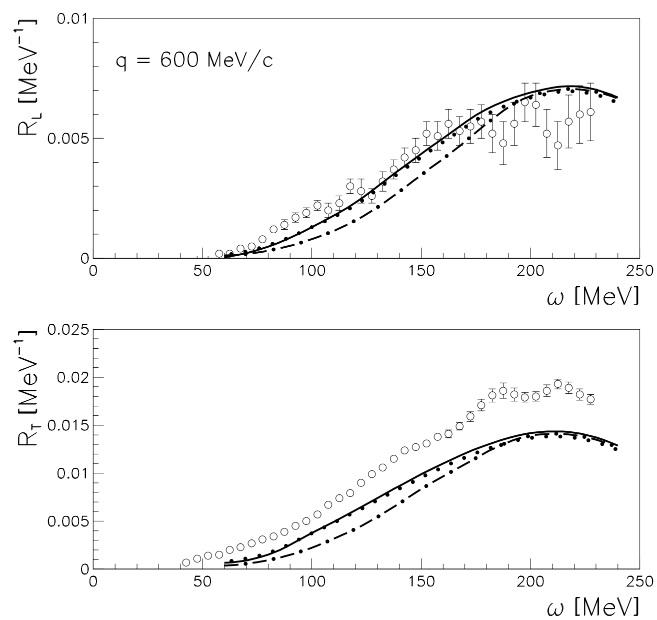

FIG. 5. The same as in Fig. 1, but for $q = 600$ MeV/c. The data are from Ref. [36].

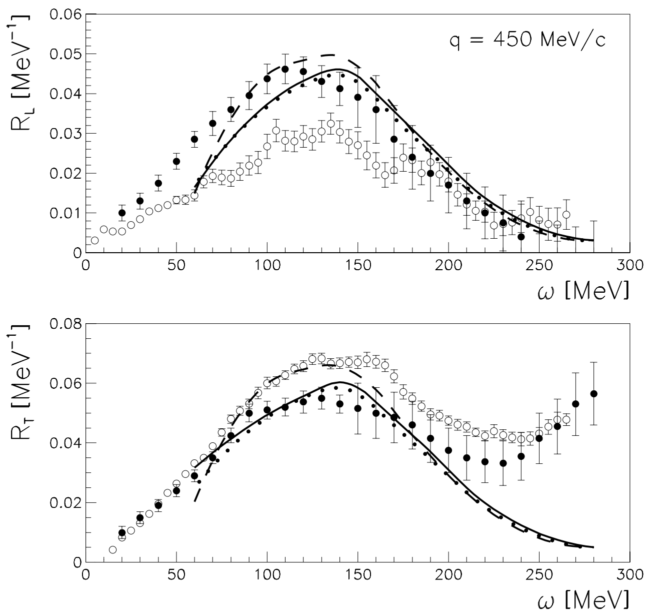

FIG. 6. Longitudinal (upper panel) and transverse (lower panel) response functions for the ^{40}Ca(e,e') reaction at $q=450$ MeV/c. The Saclay data (open circles) are from Ref. [39] and the MIT-Bates ones (black circles) are from Ref. [3]. Line convention as in Fig. 1.

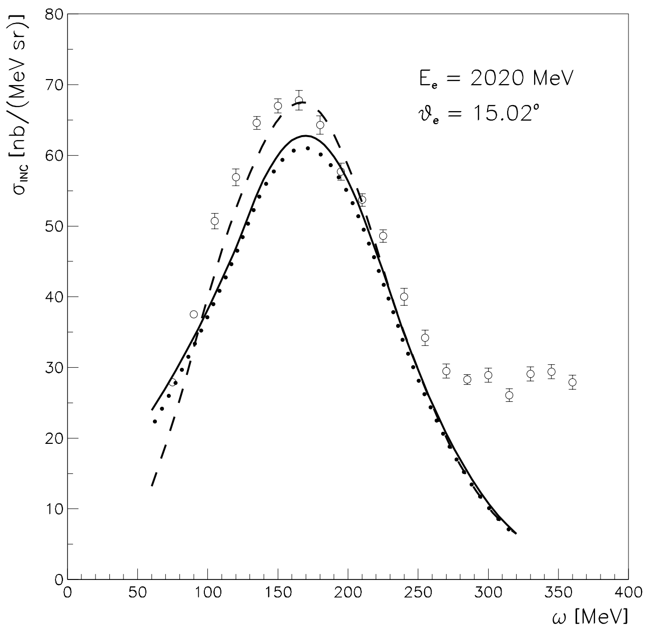

FIG. 7. The cross section for the inclusive ^{12}C(e,e') reaction at $\vartheta_e=15.02°$ and $E_e=2020$ MeV. The data are from SLAC [40]. Line convention as in Fig. 1.

the effect is negligible, and the two curves with and without the integral overlap. The effect of the inelastic channels, indicated in the figures by the difference between the complete results and the contribution from all the integrated single nucleon knockout channels, is always visible and even sizable, but it decreases on increasing the momentum transfer.

The response functions for ^{40}Ca at $q=450$ MeV/c are shown in Fig. 6 and compared with the Saclay [39] and the MIT-Bates [3] data. The results obtained with the NLSH set of parameters have been plotted, since the results with other sets are almost equivalent. The calculated response functions are of the same order of magnitude as the MIT-Bates data, while for the Saclay data the longitudinal response is overestimated and the transverse response underestimated. The factor in Eq. (68) produces an enhancement that is minimal but visible in the figure.

B. The inclusive cross section

Investigation of inclusive electron scattering in the region of large q is of great interest to provide information on the nuclear wave functions and excitation and decay of nucleon resonances. Several experiments have been carried out to explore this region. The separation of the longitudinal and transverse components of the nuclear response would be very interesting, but very difficult to perform because of the decreasing of the longitudinal-transverse ratio with increasing q. Precise measurements over a kinematical range that would allow longitudinal-transverse separation for several nuclei are, however, planned in the future at JLab, where the E-01-016 approved experiment [4] will make a precise measurement in the momentum transfer range $0.55 \leqslant q \leqslant 1.0$ GeV/c in order to extract the response functions.

In this section, we focus our attention on experimental cross sections with $\omega \lesssim 300$ MeV, since our model does not include meson exchange currents and isobar excitation contributions.

The calculated inclusive ^{12}C(e,e') cross section is displayed in Fig. 7 in comparison with the SLAC data [40] in a kinematics with a beam energy $E_e=2020$ MeV and a scattering angle $\vartheta_e \simeq 15°$. The bound state wave function has been obtained with the NLSH set. A visible enhancement is produced by the factor in Eq. (68). The effect of the integral in Eq. (61) gives a significant reduction which underestimates the data. As in the case of the transverse response of Figs. 1–6, the discrepancy might be due to two-body mechanisms which are neglected here.

In order to extend our analysis to different kinematics and target nuclei, we consider in Fig. 8 the ^{16}O(e,e') inclusive cross section data taken at ADONE-Frascati [2] with beam energy ranging from 700 to 1200 MeV and a scattering angle $\vartheta_e \simeq 32°$. The NLSH wave functions have been used in the calculations. The agreement with data is good in all the situations considered. The integral in Eq. (61) produces a reduction that is now essential to reproduce the data at 700 MeV, which correspond to a momentum transfer $q \lesssim 400$ MeV/c. Its contribution can be neglected in the other kinematics, where $q \simeq 600$ MeV/c. The effect of the factor in Eq. (68) is very small.

VII. SUMMARY AND CONCLUSIONS

A relativistic approach to inclusive electron scattering in the quasielastic region has been presented. This work can be considered as an extension of the nonrelativistic many-body

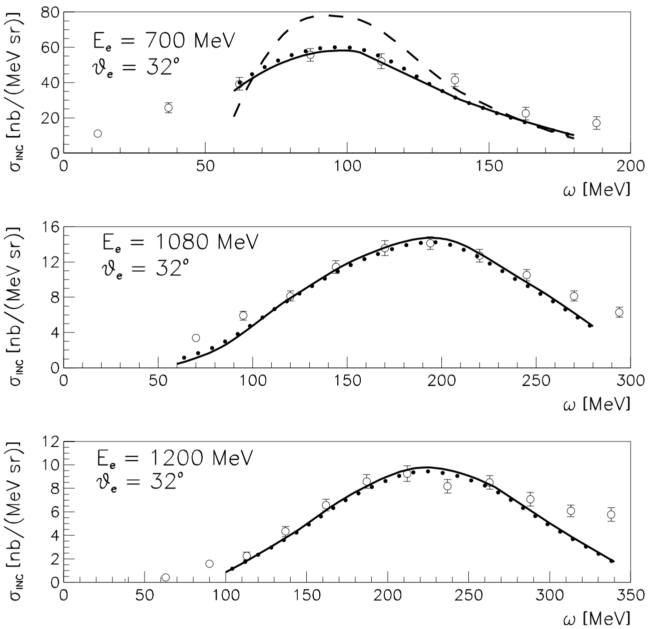

FIG. 8. The cross section for the inclusive ^{16}O(e,e') reaction at $\vartheta_e=32^o$ and $E_e=700$, 1080, and 1200 MeV. The data are from ADONE-Frascati [2]. Line convention as in Fig. 1.

approach of Ref. [15]. The components of the hadron tensor are written in terms of Green's functions of the optical potentials related to the various reaction channels. The projection operator formalism is used to derive this result. An explicit calculation of the single-particle Green's function can be avoided by means of its spectral representation, based on a biorthogonal expansion in terms of the eigenfunctions of the non-Hermitian optical potential $\mathcal{V}(E)$ and of its Hermitian conjugate. The interference between different channels is taken into account by the factor $\sqrt{1-\mathcal{V}'(E)}$, which also allows the replacement of the mean field $\mathcal{V}(E)$ by the phenomenological optical potential $\mathcal{V}_{\mathrm{L}}(E)$. After this replacement, the nuclear response functions are expressed in terms of matrix elements similar to the ones that appear in the exclusive one-nucleon knockout reactions, and the same RDWIA treatment [25] can be applied to the calculation of the inclusive electron scattering.

The effects of final state interactions are thus described consistently in exclusive and inclusive processes. Both the real and imaginary parts of the optical potential must be included. In the exclusive reaction the imaginary part accounts for the flux lost towards other final states. In the inclusive reaction, where all the final states are included, the imaginary part accounts for the redistribution of the strength among the different channels.

All the final states contributing to the inclusive reaction are contained in the Green's function, and not only those regarding one-nucleon emission. Our calculations for the inclusive electron scattering are different from the contribution of integrated single-nucleon knockout only. The difference between the two results is originated by the imaginary part of the optical potential.

The transition matrix elements are calculated using the bound state wave functions obtained in the framework of a relativistic mean field theory. The direct Pauli reduction method is applied to the scattering wave functions. Numerical results for the longitudinal and transverse response functions of ^{12}C and ^{40}Ca have been presented in comparison with data in a momentum transfer range between 400 and 600 MeV/c.

The role and relevance of the various effects of final state interactions can be different in the relativistic and nonrelativistic calculations. This is a consequence of the different features of the optical potentials in the two approaches. The final effect is, however, similar and produces qualitatively similar results in comparison with data. The relativistic framework has, however, the advantage that it can be more reliably applied to a wider range of situations and kinematics.

Our relativistic results confirm that the effects of final state interactions are large and essential to reproduce the data. The term with the integral, entering the definition of the hadron tensor $W^{\mu\mu}(\omega,q)$ in Eq. (61), gives a significant contribution, which is important to improve the agreement with data. This result is different from the one obtained in the nonrelativistic analysis [15], where this term gave only a small contribution and was thus neglected in the calculations. We stress that this term is due to the imaginary part of the optical potential, which thus produces different but important effects in the relativistic and nonrelativistic approaches. The effects of the integral in Eq. (61), as well as the difference between the complete result and the contribution of integrated single-nucleon knockout, which are both entirely due to the imaginary part of the optical potential, tend to decrease with increasing momentum transfer.

The factor $\sqrt{1-\mathcal{V}'(E)}$ is conceptually very important. It accounts for interference effects and allows the replacement of $\mathcal{V}(E)$ by $\mathcal{V}_{\mathrm{L}}(E)$. In the nonrelativistic analysis of Ref. [15], this factor produced an overall reduction of the calculated strength, which significantly improved the agreement with the experimental longitudinal response function. Only a small contribution is given by this factor in the present relativistic approach. It generally produces a small enhancement of the calculated responses, which does not significantly change the comparison with data.

Final state interactions have a similar effect on the longitudinal and transverse components of the nuclear response. In comparison with data, the longitudinal response is usually well reproduced, while the transverse response is underestimated. This seems to indicate that more complicated effects, e.g., two-body meson exchange currents, have to be added to the present single-particle approach.

The inclusive cross section for ^{12}C and ^{16}O has been calculated for momentum transfer $\lesssim$600 MeV/c. The results for ^{12}C are in agreement with those obtained for the response functions. The lack of strength in the determination of the transverse response results in an underestimation of the data. A satisfactory agreement is obtained for the ^{16}O(e,e') results.

[1] S. Boffi, C. Giusti, F.D. Pacati, and M. Radici, *Electromagnetic Response of Atomic Nuclei*, Oxford Studies in Nuclear Physics (Clarendon, Oxford, 1996), Vol. 20.
[2] M. Anghinolfi *et al.*, Nucl. Phys. **A602**, 405 (1996).
[3] C.F. Williamson *et al.*, Phys. Rev. C **56**, 3152 (1997).
[4] J.P. Chen, S. Choi, and Z.E. Meziani, JLab E-01-016.
[5] V. Van der Sluys, J. Ryckebusch, and M. Waroquier, Phys. Rev. C **51**, 2664 (1995).
[6] R. Cenni, F. Conte, and P. Saracco, Nucl. Phys. **A623**, 391 (1997).
[7] J.E. Amaro, M.B. Barbaro, J.A. Caballero, T.W. Donnelly, and A. Molinari, Phys. Rep. **368**, 317 (2002); nucl-th/0301023.
[8] A. Fabrocini, Phys. Rev. C **55**, 338 (1997).
[9] G. Co' and A.M. Lallena, Ann. Phys. (N.Y.) **287**, 101 (2001).
[10] W. Leidemann and G. Orlandini, Nucl. Phys. **A506**, 447 (1990).
[11] I. Sick, in *Proceedings of the 21st International Workshop on Nuclear Theory*, Heron Press Science Series, edited by V. Nikolaev (Heron, Sofia, 2002), p. 16.
[12] Y. Horikawa, F. Lenz, and N.C. Mukhopadhyay, Phys. Rev. C **22**, 1680 (1980).
[13] C.R. Chinn, A. Picklesimer, and J.W. Van Orden, Phys. Rev. C **40**, 790 (1989); **40**, 1159 (1989).
[14] P.M. Boucher and J.W. Van Orden, Phys. Rev. C **43**, 582 (1991).
[15] F. Capuzzi, C. Giusti, and F.D. Pacati, Nucl. Phys. **A524**, 681 (1991).
[16] F. Capuzzi and C. Mahaux, Ann. Phys. (N.Y.) **254**, 130 (1997).
[17] G.B. West, Phys. Rep. **18**, 264 (1975).
[18] G. Orlandini and M. Traini, Rep. Prog. Phys. **54**, 257 (1991).
[19] H. Feshbach, Ann. Phys. (N.Y.) **5**, 357 (1958).
[20] S. Boffi and F. Capuzzi, Nucl. Phys. **A351**, 219 (1981).
[21] F. Capuzzi, Nucl. Phys. **A554**, 362 (1993).
[22] H. Feshbach, Ann. Phys. (N.Y.) **19**, 287 (1962).
[23] F. Capuzzi and C. Mahaux, Ann. Phys. (N.Y.) **239**, 57 (1995).
[24] F. Capuzzi and C. Mahaux, Ann. Phys. (N.Y.) **245**, 147 (1996).
[25] A. Meucci, C. Giusti, and F.D. Pacati, Phys. Rev. C **64**, 014604 (2001).
[26] A. Meucci, C. Giusti, and F.D. Pacati, Phys. Rev. C **64**, 064615 (2001).
[27] E.D. Cooper, S. Hama, B.C. Clark, and R.L. Mercer, Phys. Rev. C **47**, 297 (1993).
[28] B.C. Clark, in *Proceedings of the Workshop on Relativistic Dynamics and Quark-Nuclear Physics*, edited by M.B. Johnson and A. Picklesimer (Wiley, New York, 1986), p. 302.
[29] M. Hedayati-Poor, J.I. Johansson, and H.S. Sherif, Nucl. Phys. **A593**, 377 (1995).
[30] W. Pöschl, D. Vretenar, and P. Ring, Comput. Phys. Commun. **103**, 217 (1997).
[31] G.A. Lalazissis, J. König, and P. Ring, Phys. Rev. C **55**, 540 (1997).
[32] J.J. Kelly, Phys. Rev. C **60**, 044609 (1999).
[33] T. de Forest, Jr., Nucl. Phys. **A392**, 232 (1983).
[34] A. Meucci, Phys. Rev. C **65**, 044601 (2002).
[35] P. Mergell, Ulf-G. Meissner, and D. Drechsel, Nucl. Phys. **A596**, 367 (1996).
[36] P. Barreau *et al.*, Nucl. Phys. **A402**, 515 (1983); CEA Report No. N-2334.
[37] L.R.B. Elton and A. Swift, Nucl. Phys. **A94**, 52 (1967).
[38] D.F. Jackson and I. Abdul-Jalil, J. Phys. G **6**, 481 (1980).
[39] Z.E. Meziani *et al.*, Phys. Rev. Lett. **52**, 2130 (1984); **54**, 1233 (1985).
[40] D.B. Day *et al.*, Phys. Rev. C **48**, 1849 (1993).